A PRELIMINARY ANALYSIS OF LUNAR EXTRA-MARE BASALTS: DISTRIBUTION, COMPOSITIONS, AGES, VOLUMES, AND ERUPTION STYLES

J. L. WHITFORD-STARK
Geology Dept. Sul Ross State University, Alpine, TX, U.S.A.

(Received 8 March, 1982)

Abstract. Extra-mare basalts occupy 8.5% of the lunar basalt area and comprise 1% of the total mare basalt volume. They are preferentially located where the crust is thin and topographically low. In terms of age, eruption style, and composition they are as variable as the mare basalts. In some instances extrusion in extra-mare craters was preceded by floor-fracturing whereas in other cases it apparently was not. The volume of lava erupted may have been controlled more by the volume of magma produced than by hydrostatic effects. A minimum of nearly 1300 separate basalt eruptions is indicated; the true value could be nearer 30 000 separate eruptions.

1. Introduction

Previous studies (Head, 1975; Scott *et al.*, 1977a) have illustrated that lunar mare basalts are preferentially located in topographic lows (usually impact basins) and occupy about 16% of the lunar surface area (Figure 1a). Although the majority of these basalts are found in the near side equatorial region, nearly one fifth of the total basalt area is located in the poorly studied polar and far side regions (Figure 1b). The present study characterizes the different basalt environments as delineated by units mapped by the U.S. Geological Survey as erupted basaltic materials (Wilhelms and McCauley, 1971; Wilhelms and El-Baz, 1977; Scott *et al.*, 1977b; Lucchitta, 1978; Stuart-Alexander, 1978; Wilhelms *et al.*, 1979). A few minor areas were added, whereas areas mapped as 'marets' (Beals and Tanner, 1975) and impact redistributed mafic materials (Schultz and Spudis, 1979) were omitted. The present study focuses on the basalts emplaced in extra-mare environments, that is, basalts not within the named maria (Table I) but which appear to be of the same composition as mare basalts. These extra-mare basalts comprise only about 8.5% of the total basalt area (Figure 1c), but occur within excess of 300 separate locations. Unlike the large maria where repeated eruptions and flooding of older basalts has been commonplace (Whitford-Stark, 1980a), the morphologies of basalts within these extra-mare locations can more readily be employed to determine the eruption style.

2. Distribution

The extra-mare basalts were divided into three groups; those within 'lowlands', those within floor-fractured craters, and those within unfractured craters (Figure 1d). Lowlands were defined as areas not enclosed by a single uninterrupted crater wall (or doublet) and primarily occur peripheral to the major maria or partly flood the rings of large basins.

The Moon and the Planets **26** (1982) 323–338. 0165-0807/82/0263-0323$02.40.

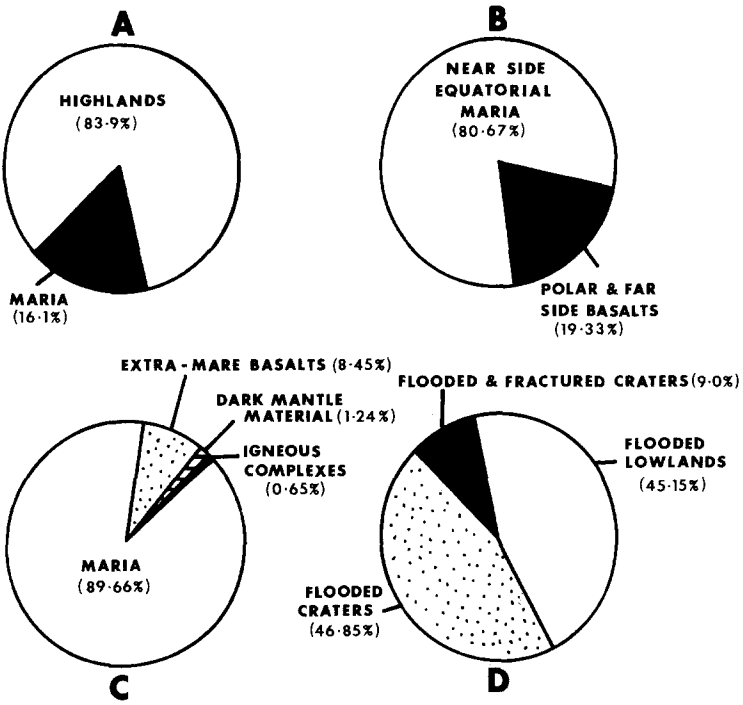

Fig. 1. Pie-graphs showing the percentage areas of basalts in different environments. The scale progressively decreases from A to D.

Figure 2 illustrates the distribution of mare basalts and includes the outlines of far side and polar impact basins and the contour of mean lunar radius of 1737.42 km derived from a global harmonic topographic model by Bills and Ferrari (1975). A previous study by Scott *et al.* (1977a) noted that most of the far side basalts were located in old impact basins though some basins (e.g., Korolev, Hertzsprung, and Mendeleev) exhibit no surface evidence of past basaltic volcanism. Additionally, Schultz and Spudis (1979) found few dark halo craters of impact origin within far side basins. These dark halo craters are interpreted by them to excavate mafic materials from beneath later ejecta deposits. The absence of such craters on the lunar far side would imply that mafic materials have been buried by a substantial thickness of material which impact craters have been unable to penetrate, that volcanism did not take place, or that the products of volcanism were of different composition to mare basalts. If mafic material were present at depth within basins such as Korolev, it would have been excavated by the large (>35 km diam) craters superimposed on that basin. On the basis of gamma-ray data, Spudis (1979) has suggested that far side volcanism may have been of KREEP composition, particularly since a radioactive high occurs in the Van de Graaff region. Limited surface coverage of the Apollo orbiter groundtracks precludes definition of the extent of such KREEP-rich materials, and extensive surface

TABLE I

The surface areas of basalts within named near side equatorial lunar maria listed in order of decreasing size.

Name	Basalt area (km^2)
O. Procellarium	1 692 000
M. Imbrium	1 130 000
M. Tranquillitatis	436 000
M. Serenitatis	353 400
M. Crisium	228 000
M. Fecunditatis	220 000
M. Insularum	110 200
M. Humorum	84 500
M. Nectaris	84 100
M. Undarum and M. Spumans	55 000
L. Somniorum	47 300
S. Aestuum	39 600
L. Mortis	34 000
M. Vaporum	32 400
P. Epidermiarum	21 150
S. Medii	18 000
P. Somnii	17 500
P. Putredinis	8 350
M. Anguis	8 150
Total	4 619 850

modification by impact events precludes definition of early KREEP volcanism by morphologic criteria.

Table II lists the areas of basalts within far side and polar basins and shows that there is no correlation between basalt area and basin size or age. Extensive areas of basalt are found only within the topographically low South Pole-Aitken and Australe basins. Although there is some degree of correspondence between far side basalt location and the areas of thin crust determined by Bills and Ferrari (1977), the match is not perfect. For example, Bills and Ferrari (1977) show an area of far side crust centered at approximately 30° N, 150° W which is as thin as the crust beneath some near side maria, but no surface basalts have been identified at that location. The distribution of far side basalts therefore appears to have been controlled by a combination of both a thin crust and the presence of a topographic low.

3. Composition of Extra-mare Basalts

Only comparatively large expanses of basalt are amenable to compositional analysis from orbital remote-sensing data because of the wide field of view of the instrumentation. Table III presents the gamma and X-ray data derived for a few large craters and some comparative analyses of returned lunar samples. The Mg/Si values for the floors of Archimedes and Tsiolkovsky are comparable to mare basalts though the Al/Si values are

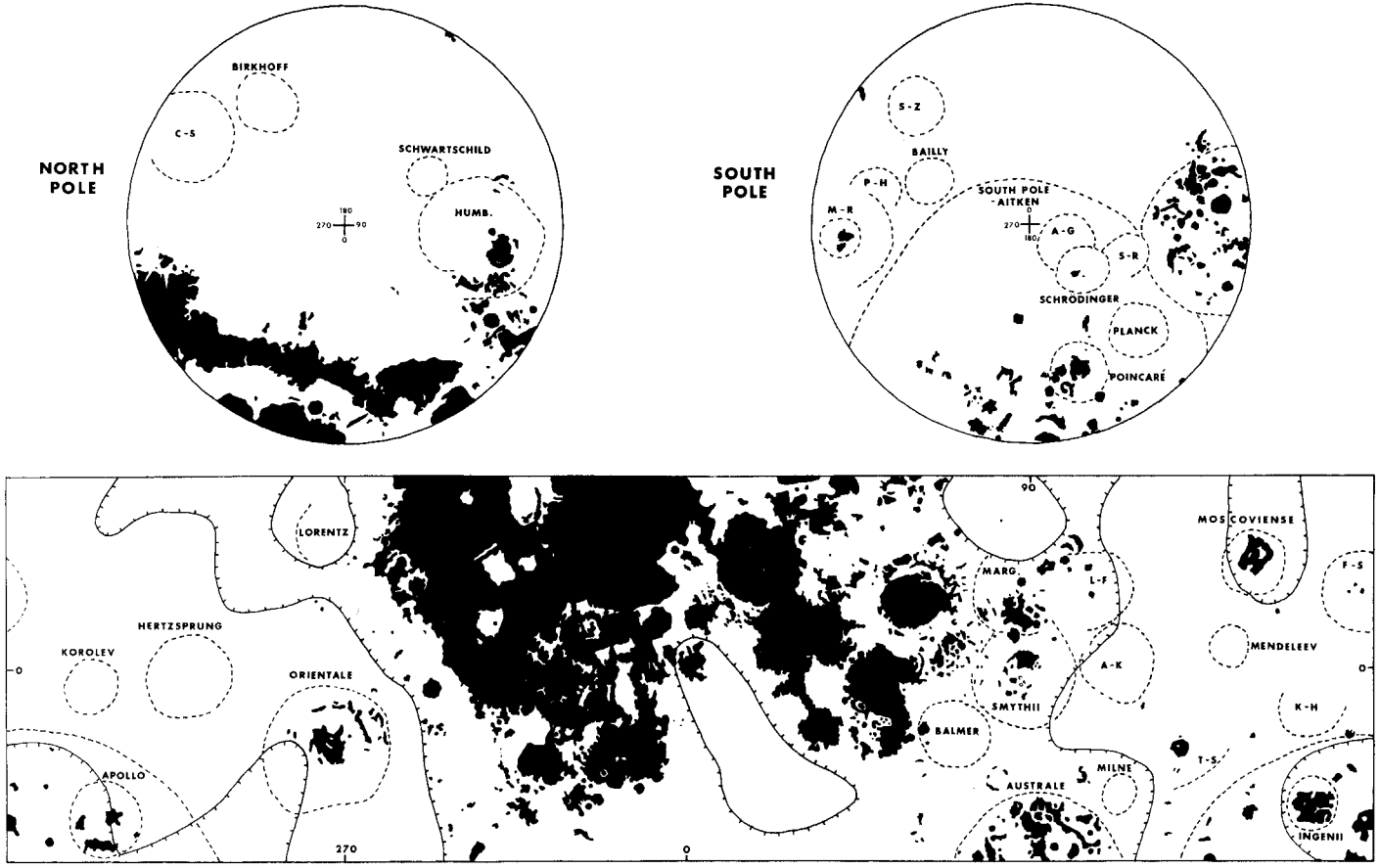

Fig. 2. Map showing the distribution of mare basalts (dark shading) on the surface of the Moon. Also shown in dashed lines are the outlines of large impact basins on the far side and polar areas (after Wilhelms, 1980). The solid lines with ticks in the equatorial region are the contours of mean lunar radius of 1737.42 km (after Bills and Ferrari, 1975); areas below the mean radius are on the ticked side of the lines. Abbreviations for basins are C-S is Coulomb-Sarton, Humb. is Humboldtianum, S-Z is Schiller-Zucchius, P-H is Pingré-Hausen, M-R is Mendel-Rydberg, A-G is Amundsen-Ganswindt, S-R is Sikorsky-Rittenhouse, L-F is Lomonosov-Fleming, A-K is Al Khwarizmi-King, T-S is Tsiolkovsky-Stark, K-H is Keeler-Heaviside, and F-S is Freundlich-Sharanov.

TABLE II

Far side and Polar basalts within maria and basins listed in order of decreasing size. Also listed are the basin sizes and ages taken from Wilhelms (1980). Areas marked * have been excluded from the total since they occur within the South Pole-Aitken basin. Note that there is no apparent correlation between basin size, age and area of basalt.

Basin/mare name	Basalt area (km²)	Age	Basin diam (km)	% of basin covered by lava
Frigoris	320 000	–	–	–
Australe	319 000	pN	880	55.5
South Pole-Aitken	190 725	pN	2500	3.9
Orientale	69 500	I	930	10.2
Marginis	64 900	–	580	24.6
Smythii	51 950	pN	840	9.4
Ingenii	36 000*	pN	560 (320)	14.6 (44.7)
Humboldtianum	35 475	N	600	12.5
Poincaré	23 750*	pN	340	26.2
Moscoviense	19 600	N	445	12.6
Apollo	18 300*	pN	505	9.1
Tsiolkovsky-Stark	12 600	–	700	3.3
Mendel-Rydberg	2 900	N?	630	0.9
Freundlich-Sharanov	1 920	pN	600	0.7
Schrödinger	1 325*	I	320	1.6
Total	1 088 570			

somewhat higher. These higher Al/Si values may result partly from sampling the walls and central peak of the crater. Excepting Grimaldi, the gamma-ray Ti values for several craters are low and comparable to low titanium basalts. These data are consistent with earth-based multispectral imaging data which also indicate low titanium values for the floor of Archimedes. Iron concentrations for those craters analyzed are low compared with returned samples and 5 to 8 wt% less than values obtained for the near side maria (Davies, 1980). The high Th values of Archimedes and Van de Graaff probably result from sampling of local KREEP materials in the crater ejecta blankets (Metzger *et al.*, 1979).

Earth-based multispectral imaging and spectral reflectance data (Johnson *et al.*, 1977; McCord *et al.*, 1976; Pieters, 1978) enables determination of TiO_2 compositional variations over a larger area of the lunar near side than that possible from orbital measurements. Spectra and images of both Archimedes and Plato indicate low titanium concentrations whereas images of other craters, such as Billy and Grimaldi, are consistent with high titanium concentrations. This preliminary analysis would indicate that the extra-mare basalts are as variable in composition as the mare basalts.

4. Ages of Extra-mare Basalts

The isolation of many extra-mare basalts makes it difficult to assign them a place in the lunar stratigraphic column. On U.S. Geological Survey maps the basalts are assigned either an Eratosthenian or Imbrian age (e.g., Wilhelms and McCauley, 1971) which

TABLE III

Compositional data derived for craters from orbital and earth-based remote-sensing and some comparative analyses of lunar samples. (1) Bielefeld (1977), (2) Adler *et al.* (1973), (3) Haines *et al.* (1978), (4) Wanke *et al.* (1975), (5) Davies (1980), (6) Metzger *et al.* (1977), (8) Johnson *et al.* (1977), (9) Pieters (1978).

Name	Mg/Si	Al/Si	Fe (wt%)	Th (ppm)	Ti (wt%)	Ti (wt%)	TiO_2 (wt%)	Spectra
Archimedes	0.19[1]	0.35[1]	9.0 ± 1.7[5]	6.7 ± 0.5[6]	0.5 ± 0.6[7]	0.8 ± 0.9[5]	2–3[8]	LIG[9]
Van de Graaff	–	–	6.6 ± 1.3[5]	2.7 ± 0.3[6]	0.6 ± 0.5[7]	0.6 ± 0.7[5]	–	–
Tsiolkovsky	0.18[2]	0.39[2]	7.1 ± 2.8[5]	0.4 ± 0.1[6]	1.4 ± 1.1[7]	1.5 ± 0.7[5]	–	–
Grimaldi	–	–	5.4 ± 1.1[5]	1.4 ± 0.2[6]	2.3 ± 0.8[7]	3.0 ± 1.1[5]	–	–
Plato	–	–	–	–	–	–	2–6[8]	LIG[9]
Neper	1.10[2]	–	–	3.4[3]	–	–	–	–
Posidonius	–	–	–	–	–	–	0–3[8]	–
Apollo 15 basalt	0.14[4]	0.21[4]	14.9[4]	0.43[4]	9.90[4]	–	–	LIG[9]
Apollo 17 basalt	0.29[4]	0.25[4]	15.0[4]	0.24[4]	7.46[4]	–	–	HDWA[9]
Anorthosite	0.02[4]	0.90[4]	0.18[4]	–	0.01[4]	–	–	–

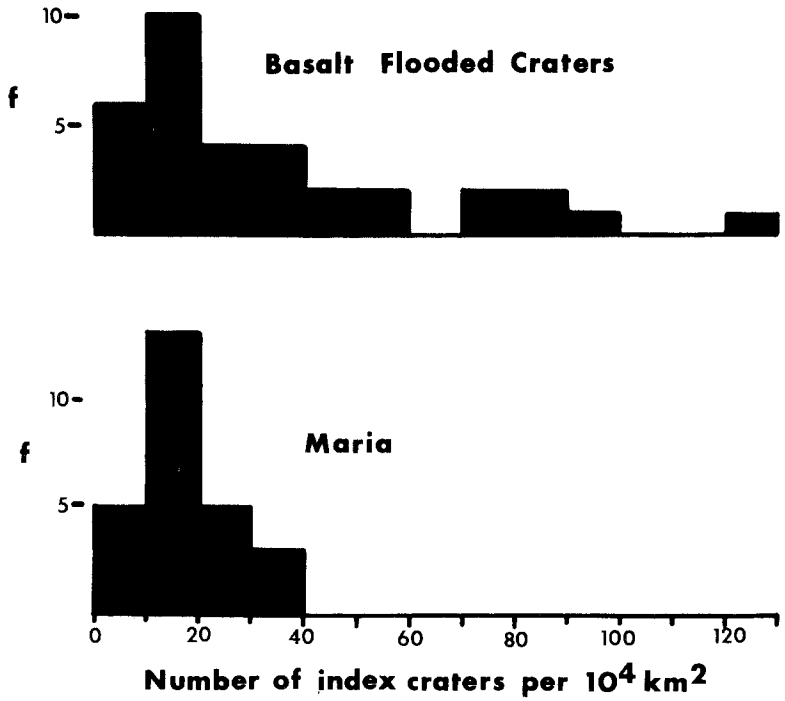

Fig. 3. Frequencies (f) of craters larger than 2 km diam as a function of the number of craters per 10^4 km^2 in lunar maria and flat-floored craters. The original data were selected from the work of Beals and Tanner (1975). Note that the peaks for the flat-floored and flooded craters and the maria are coincident but that the flooded craters extend over a wider index crater number (age) range. A higher index crater number indicates a greater age. Reasons for the differences in the two histograms are discussed in the text.

encompasses an eruption period of nearly two billion years (Whitford-Stark, 1980b). Beals and Tanner (1975) have performed crater counts for the floors of flat-floored craters and some of their data is presented in Figure 3. The histogram for flooded craters includes only the Beals and Tanner's data for craters mapped by the U.S. Geological Survey as having basaltic extrusives on their floors. The histogram for the maria exhibits a strong peak in crater frequency (number of craters equal to or greater than 2 km diameter per 10^4 km^2) of 10 to 20. Although the flooded craters exhibit a similar peak, the measured frequencies extend to much higher values. This later feature could result from the misidentification of secondary craters, the inclusion of unflooded parts of the floor within partially flooded craters, or the fact that the average values for the maria were employed by Beals and Tanner whereas in reality the age range in the surface materials of a particular mare is quite large (e.g., Whitford-Stark and Head, 1980).

In summary, the data show that the age variation of the extra-mare basalts is at least as large as that of the maria basalts. This is supported by the fact that crater basalts are both fractured by graben (e.g., Palmieri; 29° S, 48° W) and flood graben (e.g., Grimaldi; 5° S, 68° W). Graben production in the area of these craters is believed (Whitford-Stark

and Head, 1980) to have terminated about 3.6 ± 0.2 b.y. ago. In fact, the majority of the circum-Procellarum basalts post-date graben production and support the hypothesis that the locales of basalt eruption migrated outward from the mare boundaries in the later stages of mare evolution (Solomon and Head, 1980).

5. Volumes of Extra-mare Basalts

Calculation of the volumes of extra-mare basalts is subject to great uncertainty because of the difficulties in determining the basalt thickness. In a study of the fill within Mare Spumans and Mare Undarum, De Hon (1975) calculated an average basalt thickness of 200 m with local lensing up to 900 m. Employing a different technique, Whitford-Stark (1979) estimated an average thickness of 750 ± 250 m for the basalt fill within craters within Mare Australe. Employing the same technique, Whitford-Stark and Hawke (in preparation) estimated that the basalt fill within the crater Tsiolkovsky is less than 500 m thick and probably of the order of 250 m thick. Gaddis and Head (1981) have estimated an average thickness value of approximately 200 m for the basalts within and around the Orientale basin with a maximum thickness value of 600 m for the fill within Grimaldi.

Employing an average thickness value of 200 m and the total area of extra-mare basalts, a volume of approximately 1.03×10^5 km^3 is obtained. This represents only 1% of the estimated (Head, 1975) total volume of mare basalts on the Moon.

6. Mechanisms of Eruption

An analysis of floor-fracture craters by Whitford-Stark (1974) showed them to be preferentially located near the boundaries of the large maria. A more detailed analysis by Schultz (1976) led him to propose that floor fracturing was a result of sub-floor intrusions. Dvorak and Phillips (1978) have questioned the ability of a dense sub-surface basalt to produce the observed gravity anomalies associated with floor-fractured craters. However, the model which Dvorak and Phillips employed has been shown to be possibly inapplicable (Orphal, 1979). Furthermore, the craters Humboldt and Petavius which were analyzed by Dvorak and Phillips (1978) both have associated extrusive materials on their floors; extruded materials have a greater influence on the gravity field than an equivalent volume of buried materials (e.g., Schultz, 1976). The present author therefore concurs with Schultz (1976) in interpreting floor-fractured craters as being volcanically modified impact craters.

A simplified developmental sequence of intrusion and basalt flooding, similar to that of Schultz (1976), is illustrated in Figure 4. The crater Harpalus represents a fresh impact crater with a central peak. It must be remembered, however, that the host impact craters exhibited varying degrees of degradation at the time of basalt flooding. Moving downwards to the left, the crater Damoiseau represents the first stage of modification in being an unflooded floor-fractured crater. Note particularly the increase in floor/wall ratio resulting from uplift of the crater floor (Schultz, 1976). Alphonsus is representative of

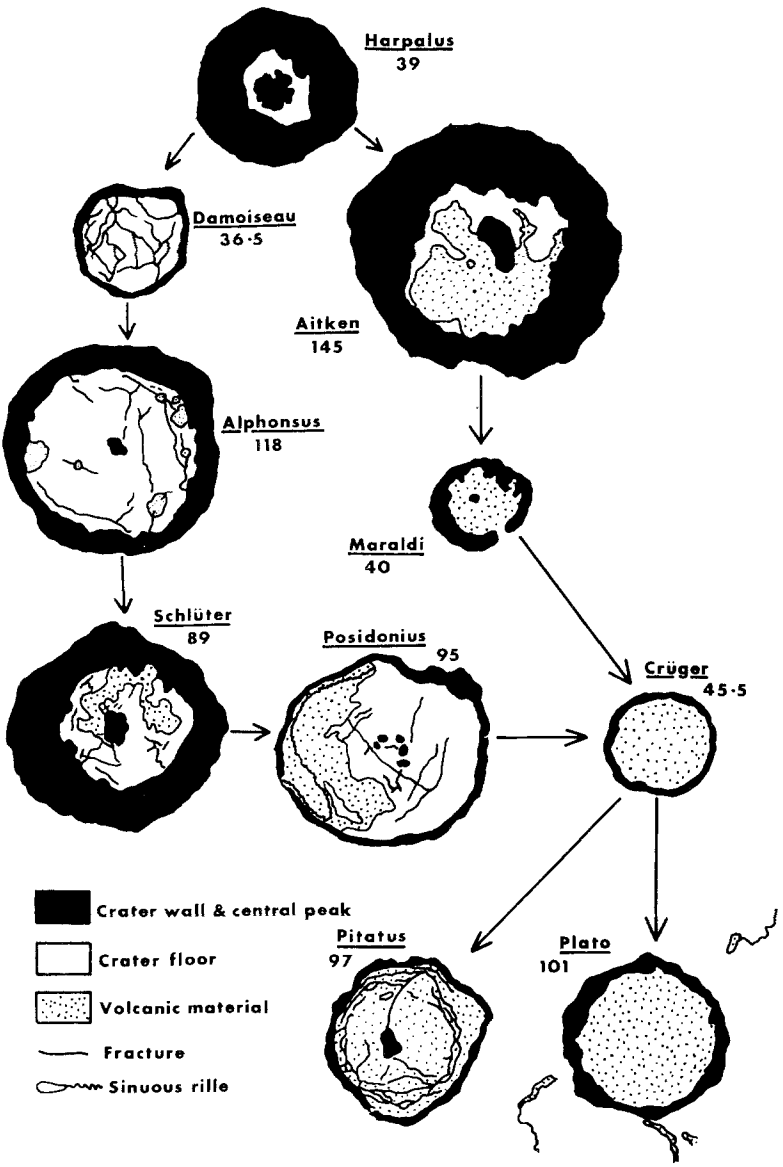

Fig. 4. Cartoon illustrating the filling of craters by mare basalts. Two scenarios are shown. Beginning with Harpulus – a fresh, unflooded impact crater – the left side of the cartoon shows the development of floor fractures (Damoiseau) and their gradual flooding (Alphonsus, Schlüter, Posidonius) until the floor is completely buried (Crüger). The right-hand side of the cartoon (Harpalus, Aitken, Maraldi, Crüger) illustrates progressive flooding of the crater floor without prior fracturing. Further volcanism takes place exterior to the crater rim (Plato) and further vertical movements may fracture the basalt floor (Pitatus). The craters are not drawn to scale; the number under the crater name is the rim crest diameter.

the third stage where volcanic material breaks through to the surface and produces dark halo craters of pyroclastic material (Head and Wilson, 1979). Further basalt eruption leads to partial flooding of the crater floor as seen in Schlüter. Prolonged eruption(s) leads to increasing proportions of the crater floor being flooded (Posidonius) until eventually the entire pre-eruption crater floor is covered by basalt (Crüger). An additional scenario is illustrated on the right-hand side of Figure 4. Beginning again with Harpalus, the next crater Aitken is partially flooded but shows no sign of fracturing and little evidence for floor uplift. Complete flooding of all pre-eruption fractures would seem to be unlikely. Further flooding of the crater would lead to just the central peak remaining above the level of the lava (Maraldi) and finally would again reach the Crüger stage. Unfortunately, once the crater floor has been covered by even a thin layer of basalt, it is impossible to tell whether such eruptions were preceded by fracturing. The absence of any floor-fractured craters surrounding the many floor-flooded craters in Mare Australe (excepting the large Humboldt and Schrödinger) lends support to the process of flooding without prior fracturing. Rather than continued flooding until the crater rim is breached, further volcanism occurs exterior to the crater rim (Plato). The only craters which appear to have been completely buried by lavas – the so-called 'ghost' craters – can be interpreted as having their fill derived from an external source.

After flooding, further vertical motions of the crater floor can result in the production of fractures (e.g., Pitatus). It is unclear whether such fractures are the product of post-eruption uplift or subsidence. The fact that all craters in which the basalt fill entirely covers the central peak are unfractured (e.g., Plato, Crüger, Archimedes, and the Australe craters) suggests that uplift is the fracture-producing mechanism. This is because the thicker fill in such craters would more favour downwarping than in the lesser flooded craters. The author could find only two craters (Maraldi and Neper) in which all but the central peak had been flooded but which did not appear to contain post-eruption fractures. Even in these two examples, the poor imagery available to the author would not preclude their presence. The presence of post-eruption fractures may therefore result from some form of interaction between the basalt fill and the central peak. Such an interaction terminated when the central peak had been sufficiently buried.

The data presented here and by Schultz (1976) illustrates that eruption of extra-mare basalts into craters can take place with or without floor uplift. Furthermore, a crater adjacent to a flooded crater may exhibit no evidence of past volcanism. Such relationships may result from differences in the pre-eruption competency of the pre-eruption floor materials or variations in the eruption style. The presence of sinuous rilles within partly flooded, fractured craters (Posidonius), partly flooded, unfractured craters (Schickard) and completely flooded craters (Ulugh Begh A), suggests that the pre-eruption floor competency is the important controlling parameter. This is supported by the fact that the basalts in flooded lowlands do not appear to be associated with fracture networks. One proposal, by Hall *et al.* (1981), is that viscous relaxation of the crater floor

was the controlling process and that the variable effects of such a process arose from pronounced spatial and temporal variations of crustal and upper mantle temperatures.

7. Style and Evolution of Extra-mare Eruptions

A detailed analysis of the Alphonsus dark halo craters by Head and Wilson (1979) led them to conclude that such features were most probably the result of a vulcanian eruption style of high gas content (several thousand ppm). The criteria for distinguishing between volcanic and impact dark halo craters are listed by Head and Wilson (1979). Volcanic dark halo craters are common on the floors of floor-fractured craters and, on the basis of the model described here, may represent the initial phases of eruption which may change to effusive lava production as the volcanic episode progresses. Lava effusion would readily bury the thin (< 50 m thick; Head and Wilson, 1979) dark halos.

Near infrared spectra of a number of volcanic dark halo deposits (Hawke *et al.*, 1980) show that they are of variable composition. Those associated with the craters Atlas (47° N, 44° E) and Franklin (39° N, 48° E) appear to be titanium rich whereas those within J. Herschel (62° N, 41° W) are titanium poor. The J. Herschel halo compositions appear to be similar to nearby mare basalts whereas those in Atlas and Franklin are not. This led Hawke *et al.* (1980) to propose that the Atlas and Franklin deposits may be associated with an earlier phase of basalt eruption in the adjacent mare that has since been buried. Whitford-Stark and Head (1980) also found that the regional dark mantle deposits were associated with the early phases of lava production in Oceanus Procellarum, but none were identified with the later lavas. Wilson and Head (1981) concluded that the regional dark mantle deposits were not particularly diagnostic of either low or high magma gas contents but that the dark halo craters did require a high gas content magma. These data would suggest that the early basalt eruptions may have been volatile-enriched relative to the younger eruptions. It is, however, not possible to substantiate this interpretation since the initial eruption phases in most areas have been buried by younger materials. Likewise, although sinuous rilles appear to predominate on the younger basalt units of Mare Imbrium, once the rille population has been normalized to the exposed surface area of each unit, no age correlations are evident (Whitford-Stark, 1980a).

A number of craters and areas of flooded lowlands contain sinuous rilles. It has been argued (Hulme, 1973) that such rilles are the product of thermal erosion by lava. Employing mathematical models, Head and Wilson (1981) have specified the conditions associated with sinuous rille formation. Their data indicate that the rilles were produced under conditions of high mass eruption rate (10^5 to $\geqslant 10^7$ kg s^{-1}) from magmas with low gas contents (< 500 ppm). Detailed topographic data required to perform similar analyses are not available for the extra-mare sinuous rilles. Similar morphologies of extra-mare sinuous rilles to those analyzed by Head and Wilson (1981) do, however, suggest that similar eruption conditions prevailed at these sites. Assuming a mean thickness of 200 m for the lava within Posidonius would result in a lava volume of approximately 450 km^3.

Head and Wilson's (1981) data indicate that such a volume could easily be the product of a single eruption.

In the vast majority of cases there is no feature within extra-mare basalts which can be unequivocally identified as a vent. Such areas might also be the result of sinuous rille-style eruptions, but sinuous rilles were not produced because of the absence of a slope needed to channelize the flow. For example, the lava erupted within the crater Zupus (17° S, 52° W), described in detail by Whitford-Stark and Head (1980), contains a sinuous rille that was produced when the crater lava fill finally breached the crater wall and flowed down to a lower topographic level. Alternatively, flood-style eruptions may have taken place within craters in which the vent cannot be identified; the lava burying the vent (Whitford-Stark, 1980a).

8. Depth of Origin of Extra-mare Basalts

Both Schultz (1976) and Head and Wilson (1979) note that although extra-mare volcanic deposits occur at a wide range of elevations, they are commonly at the same level as the adjacent mare surfaces and invoke a hydrostatic model of magma rise. Wilson and Head (1981) derived the expression:

$$D_{bf} = \frac{\rho_h D_h + \rho_m D_m - \rho_1 D_m}{\rho_1} \tag{1}$$

to describe the height of basalt emplacement above the crust-mantle interface (D_{bf}) where D_h is the crustal thickness, D_m is the depth of the magma source beneath the crust-mantle interface and ρ_h, ρ_m, and ρ_1 are the densities of the crust, mantle and magmatic liquid respectively. Figure 5 shows five closely spaced areas of basalt on the lunar far side, each with basalt at a different level. This level varies by 2.4 km between Van de Graaff and Rumford. Also plotted are the contours of crust thickness derived by Bills and Ferrari (1977) which shows that the crust thins quite markedly toward the northern Van de Graaff area. Assuming that the crust, mantle, and magmatic liquid densities were 2800, 3400, and 3100 kg m^{-3} respectively and that the source region was at the same depth below the crust-mantle interface for each magma, Equation (1) would require that the craters within the 40 km thickness contour should be emplaced to a greater height than those at the 60 km contour, the reverse of the observed situation. The effects of changing the crustal thickness and magma generation depth in the hydrostatic model are shown diagrammatically in Figure 6. It can be seen that for magma to rise to a higher level in areas of thicker crust, the magma source must be at a deeper level below the crust-mantle interface than beneath areas of thin crust. This scenario would predict that the lavas in each crater were not produced from the same magma source and that the compositions of the lavas are unlikely to be the same. Alternatively, if all the basalts were derived from a depth that was sufficiently great that magma could penetrate the surface whatever the crustal thickness, then the basalts can be from the same source and have similar compositions. In the latter case it was the volume of magma

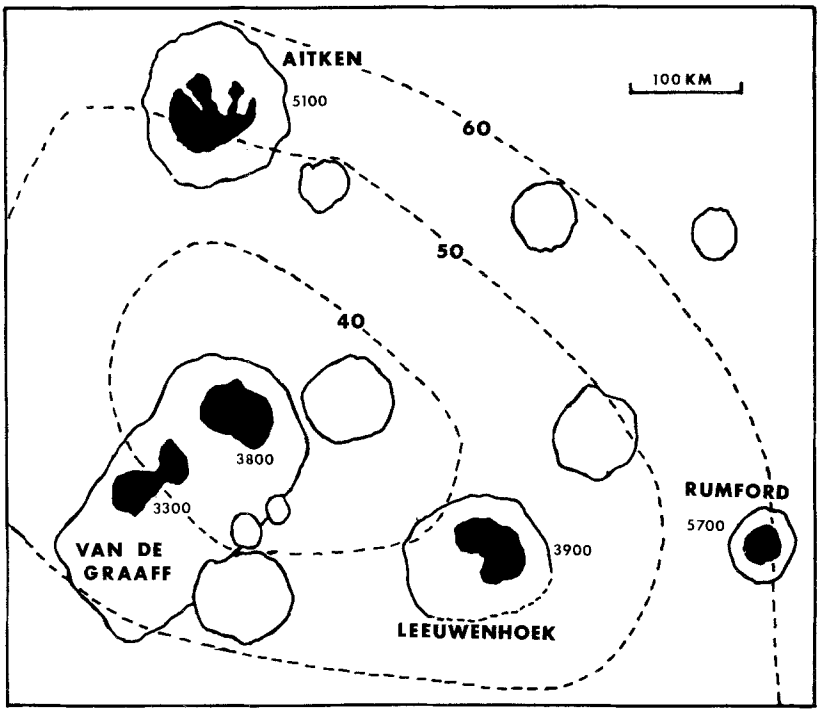

Fig. 5. Map of an area of the far side of the Moon showing the distribution of mare basalts (dark shading). The numbers next to the basalt areas are the heights of the basalt above the 1 730 000 datum. The bold numbers on the dotted lines represent the crustal thickness in kilometers (after Bill and Ferrari, 1977). Note that the height of the basalt areas increases with increasing crustal thickness.

which was produced that determined the surface basalt distribution. Such a model would be consistent with the inverse correlation between basalt height and crater diameter within the craters of Figure 5. That is, equivalent volumes of materials were produced in each eruption and the areal distribution of the basalt was determined by the pre-eruption topography.

9. Summary and Implications

Extra-mare basalts comprise approximately 8.5% of the total lunar basalt area and about 1% of the total basalt volume (excluding non-mare basalts). They are preferentially located in topographic lows and where the crust is locally thin. The extra-mare basalts are as compositionally variable as those within the maria and were emplaced over a similar time span. Eruption mechanisms within the two areas were similar.

If the depth of magma generation were sufficiently great, the amount of lava emplaced at the surface may have been controlled more by the amount of magma available than by

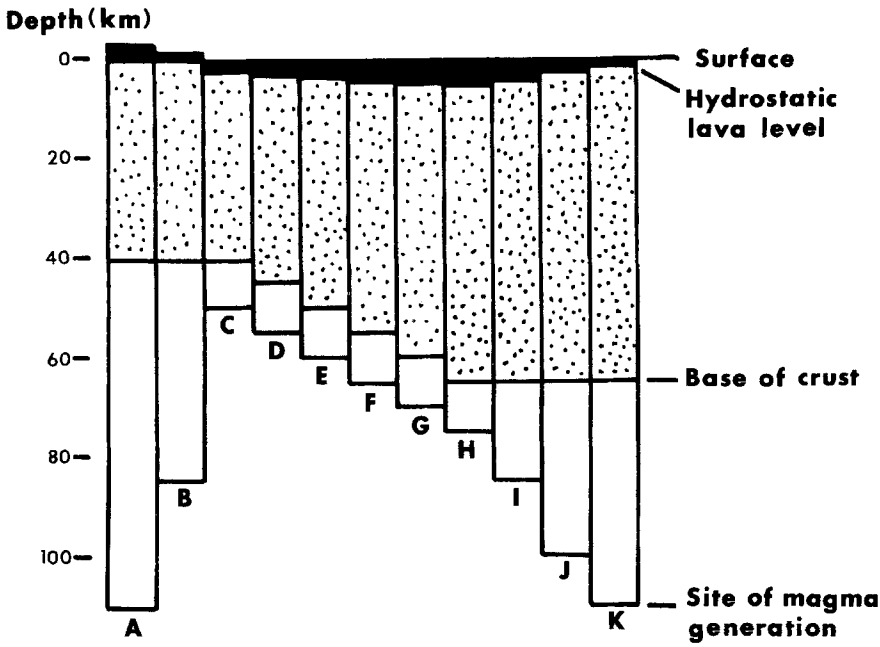

Fig. 6. Diagram showing the variation of the hydrostatic lava level as a function of crustal thickness and depth of magma generation based on Equation (1) of the text. In columns A through C the crustal thickness is constant and the depth of magma generation below the crust/mantle boundary is decreased. This results in a progressive lowering of the hydrostatic level. In columns C through H the crustal thickness is increased but the depth of magma generation below the crust/mantle boundary remains constant. This results in a further lowering of the hydrostatic level. Columns H and K again have a constant crustal thickness with progressively deepening magma generation depths below the crust/mantle boundary. Note that although magma is generated at the same depth in columns A and K, the thinner crust at A allows magma to rise above the surface whereas at K it does not reach the surface. The diagram was constructed using densities of 2800, 3400, and 3100 kg m^{-3} for the crust, mantle and magmatic liquids respectively.

hydrostatic effects. If the floor fracturing associated with unflooded craters resulted from intrusion, then the lack of extrusive features can be accounted for by a shallow magma derivation depth in the hydrostatic model. The proximity of these floor-fractured craters to the major maria suggests that the magma may have been tapped from shallow-level, sub-mare 'chambers'.

Inasmuch as each separate area of mare material must have been derived from at least one vent, the number of such areas can be employed to enable a better determination of the total number of vents that were pathways for the mare basalts. Furthermore, the average volumes of material in the extra-mare locations may provide a better idea of volumes of material in the major maria eruptive events. Table IV combines the data studied here with those derived from studies of other lunar volcanic phenomena. The number of vents recorded is probably a gross underestimate since the table does not include (1) contiguous areas of basalt of different composition which might have been

TABLE IV

Types and numbers of lunar features believed to be the product of an eruptive event. Note that for several reasons the total number of vents is probably a gross underestimate – see text for discussion. Type IVa craters are shallow, floor-fractured craters with a narrow moat adjacent to the wall. This is succeeded inward by a low-relief ridge ring. The interior floor is characteristically subdued and hummocky and the fractures, with typical polygonal or radial patterns, are subdued (Schultz, 1976). Double ring craters are small (about 8 km diameter) with an inner ring about half the diameter of the main crater (Wood, 1978).

Type of feature	Number	Reference
Isolated basalt areas	541	This paper
Mare domes	380	Whitford-Stark and Head (1977), Head and Gifford (1980)
Sinuous rilles	156	Murray (1971), Whitford-Stark (1980a)
Cones	75+	Whitford-Stark and Head (1977)
Type IVa craters	85	Schultz (1976)
Double ring craters	51	Wood (1978)
Highland domes	7	Head and McCord (1978)
Total	1296	

derived from separate vents, (2) features of volcanic origin which are unrecognized because we have no terrestrial analog, (3) vents flooded by their own or later lavas, and (4) lavas covered by later deposits. The table does, however, serve to illustrate that the lunar surface basalts were the product of multitudinous eruptions and were not derived from singular continuous outpourings. On the basis of Head's (1975) estimate of 10^7 km^3 for the total volume of lunar mare basalt and an estimate of 1200 km^3 for the average basalt volume in Mare Australe craters (Whitford-Stark, 1979), the number of vents could reasonably be increased by an order of magnitude. Because the total volume of extra-mare basalt is estimated as only about 1% of the total lunar mare basalt volume, extrapolation would indicate that the total number of separate lunar vents may have been closer to 30 000.

Acknowledgements

R. A. De Hon, P. H. Schultz, and C. A. Wood are thanked for reviews which led to improvements to the manuscript. The inspiration for this study was provided by J. W. Head. This work was completed under NASA Grant NAGW-243.

References

Adler, I., Trombka, J. I., Yin, L. O., Gorenstein, P., Bjorkholm, P., and Gerard, J.: 1973, *Naturwissenschaften* **60**, 231–242.
Beals, C. S. and Tanner, R. W.: 1975, *The Moon* **12**, 63–90.
Bielefeld, M. J.: 1977, *Proc. Lunar Sci. Conf. 8th*, 1131–1147.
Bills, B. G. and Ferrari, A. J.: 1975, *Proc. Lunar Sci. Conf. 6th*, Frontispiece.
Bills, B. G. and Ferrari, A. J.: 1977, *J. Geophys. Res.* **82**, 1306–1314.
Davies, P. A.: 1980, *J. Geophys. Res.* **85**, 3209–3224.

De Hon, R. A.: 1975, *Proc. Lunar Sci. Conf. 6th*, 2553–2561.
Dvorak, J. and Phillips, R. J.: 1978, *Proc. Lunar Planet. Sci. Conf. 9th*, 3651–3668.
Gaddis, L. R. and Head, J. W.: 1981, *Lunar Planet. Sci.* **XII**, 321–323.
Haines, E. L., Etchegaray-Ramirez, M. I., and Metzger, A. E.: 1978, *Proc. Lunar Planet. Sci. Conf. 9th*, 2985–3013.
Hall, J. L., Solomon, S. C., and Head, J. W.: 1981, *J. Geophys. Res.* **86**, 1935–1952.
Hawke, B. R., McCord, T. B., and Head, J. W.: 1980, *Reports of Planetary Geology Program-1980*, NASA TM-82385, 512–514.
Head, J. W.: 1975, *Origins of Mare Basalts*, 66–69.
Head, J. W. and Gifford, A.: 1980, *The Moon and Planets* **22**, 235–258.
Head, J. W. and McCord, T. B.: 1978, *Science* **199**, 1433–1436.
Head, J. W. and Wilson, L.: 1979, *Proc. Lunar Planet. Sci. Conf. 10th*, 2861–2897.
Head, J. W. and Wilson, L.: 1981, *Lunar Planet Sci.* **XII**, 427–429.
Hulme, G.: 1973, *Modern Geology* **4**, 107–117.
Johnson, T. V., Saunders, R. S., Matson, D. L., and Mosher, J. A.: 1977, *Proc. Lunar Sci. Conf. 8th*, 1029–1036.
Lucchitta, B. K.: 1978, *U.S. Geol. Surv. Misc. Inv. Ser.* Map I–1062.
McCord, T. B., Pieters, C., and Feierberg, M. A.: 1976, *Icarus* **29**, 1–34.
Metzger, A. E. and Parker, R. E.: 1979, *Earth Planet. Sci. Lett.* **45**, 155–171.
Metzger, A. E., Haines, E. L., Parker, R. E., and Radocinski, R. G.: 1977, *Proc. Lunar Sci. Conf. 8th*, 949–999.
Metzger, A. E., Haines, E. L., Etchegaray-Ramirez, M. I., and Hawke, B. R.: 1979, *Proc. Lunar Planet. Sci. Conf. 10th*, 1701–1718.
Murray, J. B.: 1971, in G. Fielder (ed.), *Geology and Physics of the Moon*, Elsevier, N.Y. 27–39.
Orphal, D. L.: 1979, *Lunar Planet. Sci.* **X**, 949–951.
Pieters, C. M.: 1978, *Proc. Lunar Planet. Sci. Conf. 9th*, 2825–2849.
Schultz, P. H.: 1976, *The Moon* **15**, 241–273.
Schultz, P. H. and Spudis, P. D.: 1979, *Proc. Lunar Planet Sci. Conf. 10th*, 2899–2918.
Scott, D. H., Diaz, J. M., and Watkins, J. A.: 1977a, *Proc. Lunar Sci. Conf. 8th*, 1119–1130.
Scott, D. H., McCauley, J. F., and West, M. N.: 1977b, *U.S. Geol. Surv. Misc. Inv. Ser.* Map I–1034.
Solomon, S. C. and Head,J. W.: 1980, *Rev. Geophys. Space Phys.* **18**, 107–141.
Spudis, P. D.: 1979, *Conf. Lunar Highlands Crust*, 157–159.
Stuart-Alexander, D. E.: 1978, *U.S. Geol. Surv. Misc. Inv. Ser.* Map I–1047.
Wanke, H., Palme, H., Baddenhausen, H., Dreibus, G., Jagoutz, E., Kruse, H., Palme, C., Spettel, B., Teschke, F., and Thacker, R.: 1975, *Proc. Lunar Sci. Conf. 6th*, 1313–1340.
Whitford-Stark, J. L.: 1974, *Nature* **248**, 573–574.
Whitford-Stark, J. L.: 1979, *Proc. Lunar Planet Sci. Conf. 10th*, 2975–2994.
Whitford-Stark, J. L.: 1980a, Ph.D. Thesis, Brown University, Unpublished.
Whitford-Stark, J. L.: 1980b, *J. Brit. Astron. Assoc.* **90**, 312–345.
Whitford-Stark, J. L. and Head, J. W.: 1977, *Proc. Lunar Sci. Conf. 8th*, 2705–2724.
Whitford-Stark, J. L. and Head, J. W.: 1980, *J. Geophys. Res.* **85**, 6579–6609.
Wilhelms, D. E.: 1980, *Conf. on Multi-ring Basins*, 115–117.
Wilhelms, D. E. and El-Baz, F.: 1977, *U.S. Geol. Surv. Misc. Inv. Ser.* Map I–948.
Wilhelms, D. E. and McCauley, J. F.: 1971, *U.S. Geol. Surv. Misc. Inv. Ser.* Map I–703.
Wilhelms, D. E., Howard, K. A., and Wilshire, H. G.: 1979, *U.S. Geol. Surv. Misc. Inv. Ser.* Map I–1162.
Wilson, L. and Head, J. W.: 1981, *J. Geophys. Res.* **86**, 2971–3001.
Wood, C. A.: 1978, *Lunar Planet. Sci.* **IX**, 1264–1266.